NaK Variable Conductance Heat Pipe
for Radioisotope Stirling Systems

Calin Tarau[1], William G. Anderson[2], and Kara Walker[3]
Advanced Cooling Technologies, Inc., Lancaster, PA 17601 U.S.A.

In a Stirling radioisotope power system, heat must continually be removed from the General Purpose Heat Source (GPHS) modules to maintain the modules and surrounding insulation at acceptable temperatures. The Stirling convertor normally provides most of this cooling. If the Stirling convertor stops in the current system, the insulation is designed to spoil, preventing damage to the GPHS, but also ending use of that convertor for the mission. An alkali-metal Variable Conductance Heat Pipe (VCHP) was designed to allow multiple stops and restarts of the Stirling convertor. In the design of the VCHP for the Advanced Stirling Radioisotope Generator, the VCHP reservoir temperature can vary between 40 and 120°C. While sodium, potassium, or cesium could be used as the working fluid, their melting temperatures are above the minimum reservoir temperature, allowing working fluid to freeze in the reservoir. In contrast, the melting point of NaK is -12°C, so NaK can't freeze in the reservoir. One potential problem with NaK as a working fluid is that previous tests with NaK heat pipes have shown that NaK heat pipes can develop temperature non-uniformities in the evaporator due to NaK's binary composition. A NaK heat pipe was fabricated to measure the temperature non-uniformities in a scale model of the VCHP for the Stirling Radioisotope system. The temperature profiles in the evaporator and condenser were measured as a function of operating temperature and power. The largest ΔT across the condenser was 28°C. However, the condenser ΔT decreased to 16°C for the 775°C vapor temperature at the highest heat flux applied, 7.21 W/cm². This decrease with increasing heat flux was caused by the increased mixing of the sodium and potassium in the vapor. This temperature differential is similar to the temperature variation in this ASRG heat transfer interface without a heat pipe, so NaK can be used as the VCHP working fluid.

Keywords: Alkali metal heat pipes, variable conductance heat pipes, radioisotope Stirling systems, NaK heat pipes, Advanced Stirling Radioisotope Generator, space radiator systems.
PACS: 44.30.+v, 44.35.+c.

I. INTRODUCTION

In a Stirling radioisotope power system, one or more General Purpose Heat Source (GPHS) modules supply heat to a Stirling convertor. This heat is used to generate electric power, while the waste heat is radiated to space. The maximum allowable GPHS module operating temperature is set by the iridium cladding around the fuel. The GPHS module is designed so that it will not release radioisotopes, even under such postulated events as a launch vehicle explosion, or reentry through the earth's atmosphere. However, if the iridium cladding is overheated, grain boundary growth can weaken the cladding, possibly allowing radioisotopes to be released during an accident. Once the GPHS is installed in the radioisotope Stirling system, it must be continually removed. Normally, the Stirling convertor removes the heat, keeping the GPHS modules cool. There are three basic times when it may be desirable to stop and restart the Stirling convertor:

- During installation of the GPHS
- During some missions when taking scientific measurements to minimize electromagnetic interference and vibration
- Any other unexpected stoppage of the convertor during operation on the ground or during a mission.

In the current system, the insulation will spoil to protect the GPHS from overheating. A VCHP could potentially allow convertor operation to be restarted, depending on the reason for stoppage. It would also save replacing the insulation after such an event during ground testing.

---

[1] R&D Engineer, Aerospace Products.
[2] Lead Engineer, Aerospace Products, AIAA member. Bill.Anderson@1-act.com.
[3] R&D Engineer, Aerospace Products.

A, VCHP Provides Back Up Cooling for the Stirling Radioisotope Power System

The schematics in Fig. 1a and b show the basic concept of the VCHP integrated with a Stirling convertor supplied with heat from an Isotope Heat Source. The evaporator of the VCHP is in contact with the GPHS module(s). The non-condensable gas (NCG) charge in the system is sized so the secondary radiator is blocked during normal operation and the VCHP delivers heat to the heater head; see Fig. 1(a). When the Stirling convertor is stopped, the temperature of the entire system starts to increase. In turn, the saturated working fluid vapor pressure increases as the temperature increases. This compresses the NCG. As shown in Fig. 1(b), this opens up the radiator. Once the radiator is fully open, all of the heat is dumped to the radiator, and the temperature stabilizes. Once the Stirling convertor starts operating again, the vapor temperature and pressure start to drop. The non-condensable gas expands and blankets the radiator, and the system is back to the normal state (Fig. 1(a)).
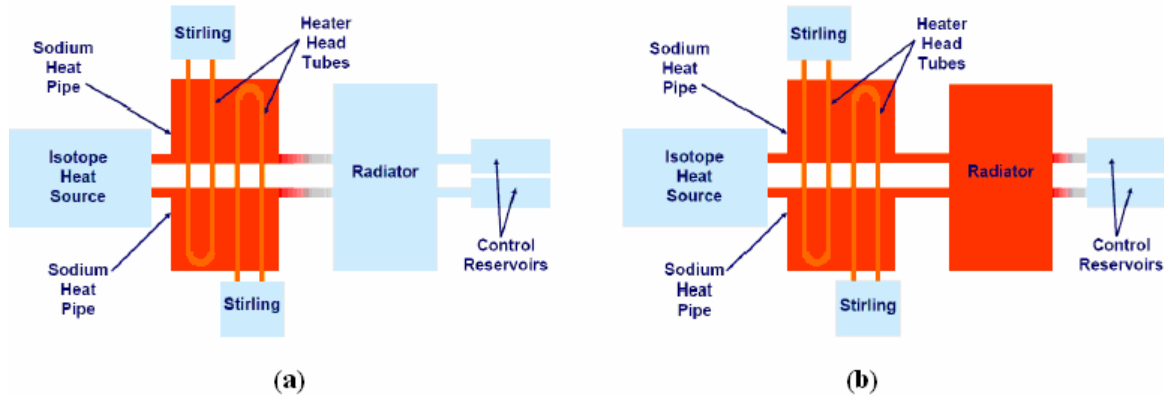

FIGURE 1. (a) Stirling convertor is operating. (b) Stirling convertor is stopped.

B. Base Line Design

The Advanced Stirling Radioisotope Generator (ASRG) (Chan, Wood, and Schreiber, 2007), with an 850°C heater head temperature, was selected as the baseline design. The system consists of two Advanced Stirling Convertors (ASCs), mounted back to back for dynamic balance. Heat to each ASC is supplied by one GPHS module. During operation, a heat collector is used to conduct the heat from the GPHS into the Stirling heater head, see Fig. 2(a). A cold-side adapter flange (CSAF), shown in Fig. 2(b) is used to conduct the waste heat from the Stirling convertor cold side to the ASRG housing. This is fabricated from copper, and serves as a structural member. The cold-end flange temperature is primarily set by the sink temperature seen by the ASRG radiating housing, which varies from earth (including launch) environments to deep space. Its operating temperature ranges from 40 to 120°C. This flange was selected as the best location for the cold VCHP reservoir as seen in Figure 3.
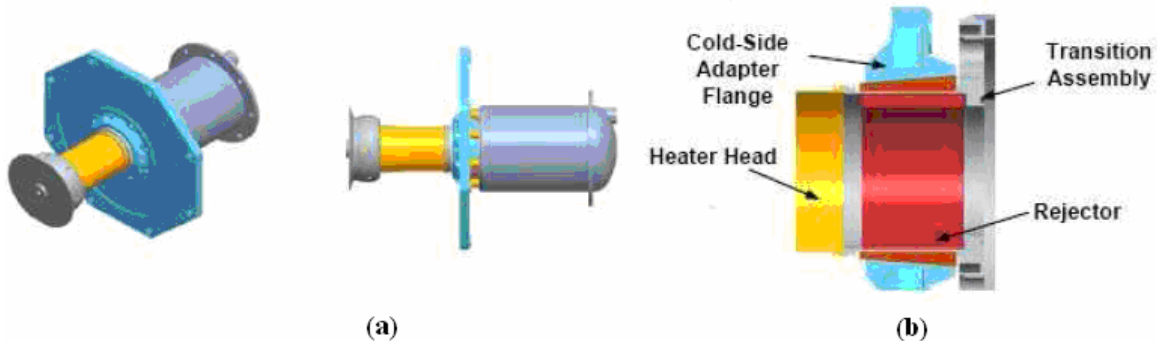

FIGURE 2. (a) Stirling Convertor with Heat Collector and Cold-Side Adapter Flange. (b) Cold-Side Adapter Flange (Chan, Wood, and Schreiber, 2007).

American Institute of Aeronautics and Astronautics

Figure 3 shows the schematic of the VCHP integration as a back up cooling system for the Advanced Stirling Convertor (ASC). In principle it corresponds to one half of the ASRG system. The heat pipe is wrapped around the existing heat collector so the original ASC configuration is not modified. The radiator is located outside the ASRG case while the reservoir is attached to the CSAF inside the case. The VCHP is designed in such a way that, during normal operation of the Stirling convertor, the working fluid vapor – NCG interface front is located inside the case (housing) to minimize the heat loss due to the presence of the VCHP. When the Stirling convertor is stopped, the NCG front is located between the upper side of the radiator and the entrance of the ASC case.
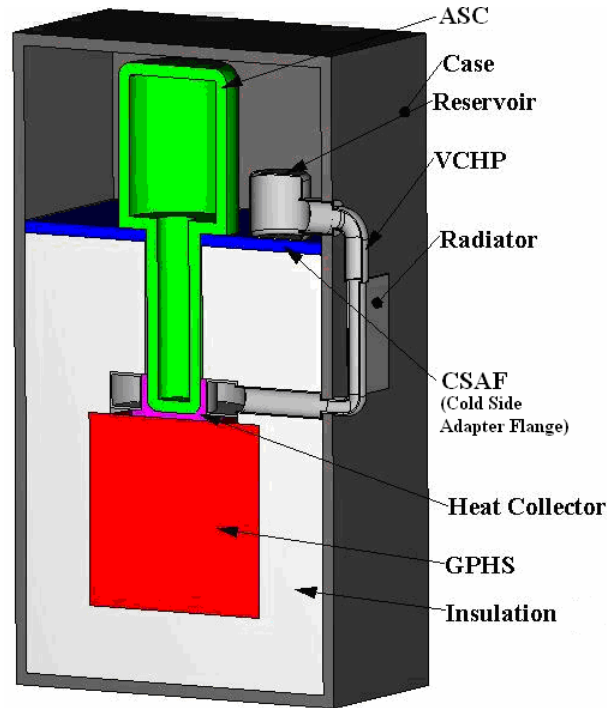

FIGURE 3. Schematic showing a cut-away of the ASRG with back-up cooling provided by a VCHP.

TABLE 1. Sodium, Potassium, Cesium, and NaK Fluid Properties at 850°C.

Property \ Fluid	Na	K	Cs	NaK
Melting Temperature, (°C)	97.8	63.2	28.4	-12.7
Boiling Temperature, (°C)	881.4	756.5	668.4	785
Vapor Pressure, (KPa)	75.99	222.9	432.65	175.29
Surface Tension, (N/m)	0.121	0.058	0.030	0.067
Liquid Viscosity, (Pa.s)	0.000162	0.000116	0.000138	0.000129
Latent Heat, (MJ/kg)	4.41	2.05	0.50	2.57

C. Heat Pipe Working Fluid

In this 850°C temperature range, there are four potential working fluids: sodium, potassium, cesium, and eutectic NaK. Eutectic NaK is a mixture of sodium and potassium (roughly 78% potassium) with a low melting point. Working fluid properties at 850°C are shown in Table 1. NaK was chosen as the baseline working fluid, since it melts at -12.7°C, which is significantly lower than either sodium or potassium. NaK is liquid over the entire range of 40 to 120°C for a

reservoir mounted on the CSAF. Ernst (2007) states that it is necessary to have the reservoir temperature above the melting point. During his alkali metal VCHP tests with reservoir temperatures below the freezing point, the entire fluid inventory ended up frozen in the reservoir. If sodium or potassium is used for this application, either the reservoir will have to be heated, or a different reservoir location will be required. NaK was chosen over cesium because its Merit number is roughly 5 times higher than cesium, and its lower, and hence, safer, melting temperature.

D. Potential NaK Temperature Non-Uniformities

NaK is a eutectic mixture with roughly 78% potassium. Unfortunately, there is no azeotropic mixture of sodium and potassium. In an azeotropic mixture, the compositions of the liquid and vapor phases are identical, so the composition of the liquid does not change during boiling. In a non-azeotropic mixture, the vapor is enriched in the component with the higher vapor pressure. In the case of NaK, the vapor is enriched in potassium when compared with the liquid. In other words, if a pool of NaK was allowed to boil away (with all of the vapor removed), the fraction of sodium in the pool would continually rise. In a NaK heat pipe, the liquid is constantly replenished, so that the compositions will remain constant. However, in some cases, it is possible for temperature non-uniformities to develop, even with a constant heat flux in the evaporator (Anderson, 1993, Anderson and Tarau, 2008).

Figure 4 shows the dew point and bubble point curves at a constant pressure of 1 atmosphere, for liquid compositions that vary from all sodium to all potassium. The vapor pressure is 1 atm. when the temperature is 758°C for a pool of pure liquid potassium. The temperature must be increased to 882°C for the vapor pressure above a pure sodium pool to reach 1 atm. At all compositions in between, the vapor potassium molar fraction ("Dew Point Curve") is higher than the liquid potassium molar fraction ("Bubble Point Curve"). Eutectic NaK contains 0.675 mole fraction of potassium. As shown in Fig. 4, the temperature is 786°C when the pressure is 1 atm. A tie line is shown in Fig. 6 between eutectic liquid NaK and its equilibrium vapor composition. Note that the vapor is enhanced in potassium when compared with the liquid, with a 0.874 mole fraction potassium.
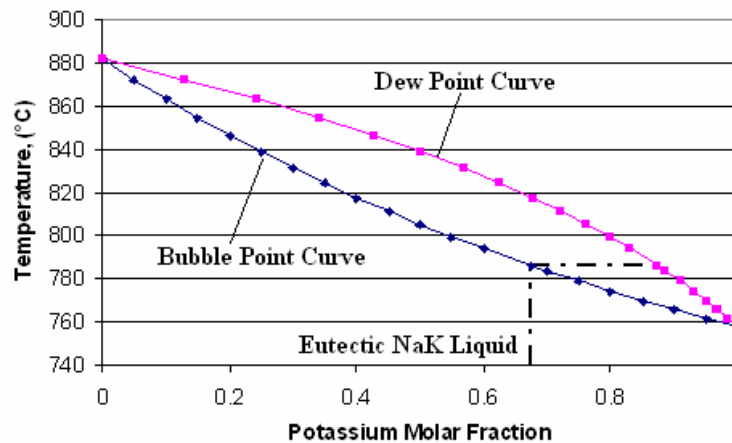

FIGURE 4. Dew point and bubble point curves for NaK vapor and liquid at a constant pressure of 0.1MPa.

As discussed in Anderson (1993), the variation of the liquid composition can give rise to a temperature variation. The pressure in the vapor space is constant, assume 1 atm. The liquid composition at the start of the evaporator wick will be eutectic NaK, so the vapor temperature would be 786°C. At the end of the evaporator wick furthest from the condenser, the composition is somewhere between eutectic NaK and sodium. If we assume that the composition at the end is pure sodium, the temperature there would be 882°C to boil off the pure sodium at the same pressure, which is almost 100°C higher. The actual temperature variation will depend on a number of things, including how much the liquid composition changes, and how much the vapor is mixed in the evaporator.

Anderson (1993) conducted tests on a NaK heat pipe with a series of thermocouple wells to measure the temperature non-uniformities. He found that when the artery was active, uniform heat fluxes in the NaK pipe could generate 80°C temperature non-uniformities with a 30 W/cm^{2} heat flux. The temperature difference decreased to roughly 50°C as the heat flux was increased to 53 W/cm^{2}, probably as a result of increased vapor mixing. These conclusions were in agreement with the later experiments developed by Anderson and Tarau (2008). A roughly 70°C

temperature difference was measured in the 0.12 m long evaporator of a NaK VCHP designed and tested as proof of concept for the ASRG VCHP application. This case was also characterized by a constant heat flux heat input.

The heat path from the GPHS module to the Stirling convertor's working fluid consists of heat collector, heater head wall and internal heat exchanger; see Figure 5 below. It is highly desirable that the temperature non-uniformity developed along the heat collector – heater head interface (heat transfer interface) is minimized, which allows a higher Stirling convertor efficiency. Currently, when no back up cooling VCHP is installed, the temperature difference at the above mentioned interface is around 17°C, based on ACT's system thermal analysis. If a single component working fluid VCHP was installed this temperature difference would be reduced, since the VCHP would have a nearly constant vapor temperature. However, a NaK heat pipe will have temperature differences due to its binary composition. Previous NaK heat pipes have had temperature differences of up to 70-80°C. A NaK heat pipe would not be suitable to cool the Stirling convertor with this high temperature non-uniformity. There are several factors that will reduce the temperature difference in the current application when compared with previous NaK heat pipes:

- Previous systems used a constant heat flux, while the current system uses constant power.
- The heat pipe lengths in previous systems tested were larger (~ 0.11 – 0.13 m) than in the current system
- Higher heat flux in the current case
- The temperature difference in previous tests was measured at the evaporator, while in the current system the region of concern is the condenser.

We believe that at least the first three dissimilarities are favorable to smaller temperature non-uniformities development at the VCHP-heater head interface in the ASRG system. This paper presents an experimental investigation on NaK behavior where the heat transfer conditions are similar to those in an ASRG with VCHP.
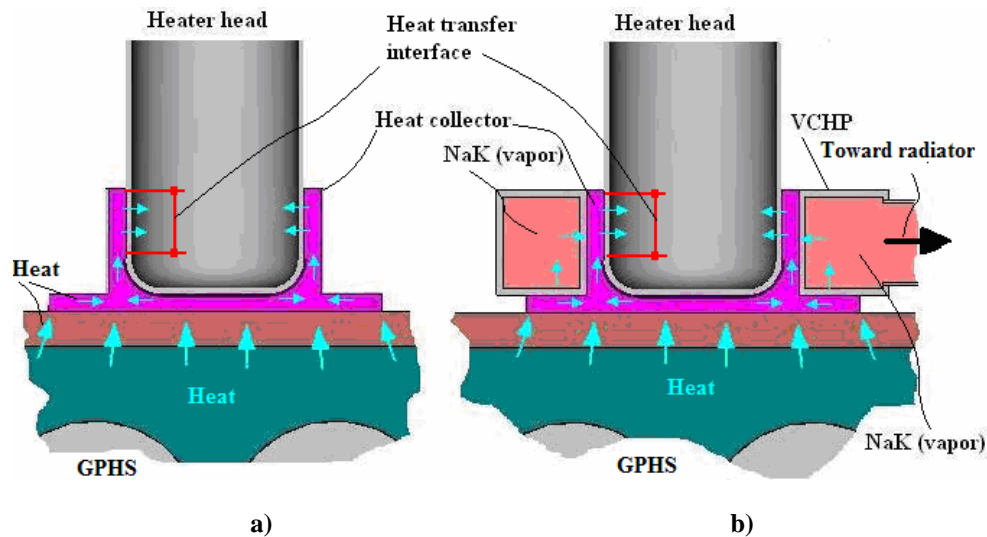

FIGURE 5. Heat path from the GPHS module to the heater head's working fluid during ASC normal operation when a) no VCHP is installed and b) VCHP is installed as backup cooling system.

II. EXPERIMENTAL NaK BEHAVIOR TEST SETUP

The experimental NaK behavior test setup was designed to determine temperature distributions in both wall and vapor at the heat transfer interfaces of the evaporation and condensation regions. A picture of the test setup is shown below in Fig. 6.
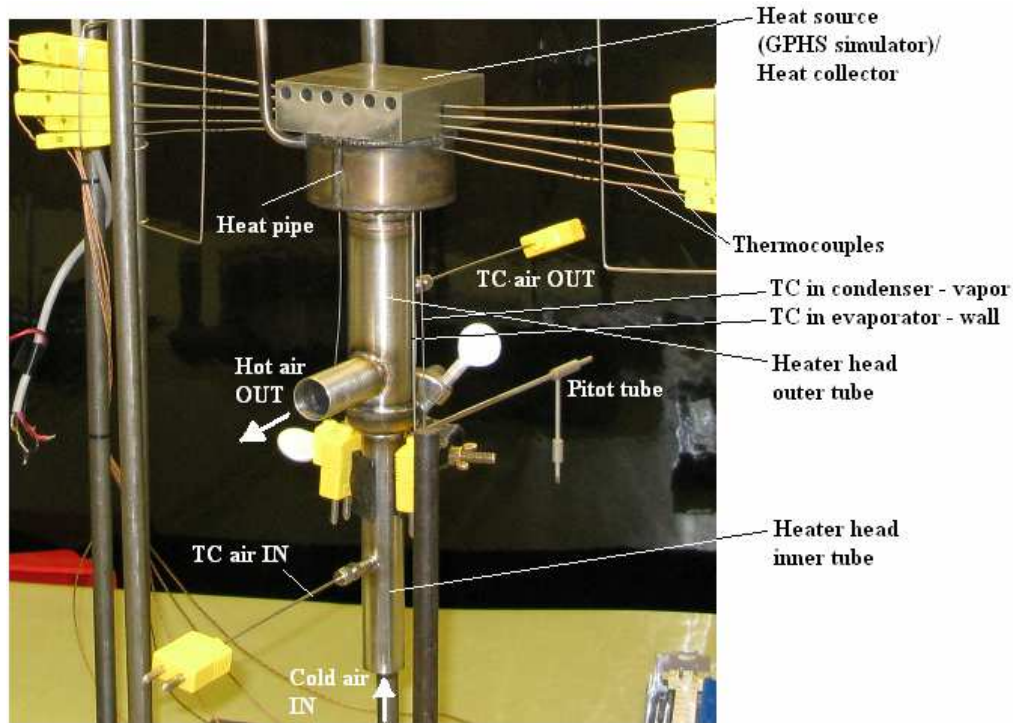
FIGURE 6. NaK behavior test setup – external details.

The test setup contains a rectangular heat source (GPHS simulator) supplying heat to a "donut" shaped heat pipe which in turn is cooled from the inside surface by a heater head simulator. For this experiment, the GPHS, heat collector and the inner wall of the heat pipe are simulated together by a nickel (Ni 201) heater block with 6 cartridge heaters. The cartridge heaters are inserted into the main body without brazing. The material of the outer wall of the heat pipe is stainless steel 304 (SS304). The heater head is simulated by two SS304 tubes concentrically assembled to form an annular space. As seen in Fig. 6, the heat pipe is cooled by a gas (air) entering through the inner tube of the heater head simulator, passing adjacent to the heat pipe, and then exhausted to the room.

In the real case of an ASRG with VCHP installed (Figure 5 b), the heat would be conducted through three walls from the vapor to the working fluid (helium) inside the heater head: VCHP wall (Haynes 230), heat collector wall (Nickel 201) and heater head wall (MarM 247). The experimental setup used a single Nickel 201 wall for simplicity, and to better control the thermal resistance between the vapor and coolant.

Temperature profiles are obtained by symmetrical measurements on two sides of the test setup using thermocouples (K Type) that are moved in their TC wells; see Figure 7. Referring to the right side of Figure 7, the purpose of each thermocouple can be described as follows:

- Thermocouples from 1 to 3 measure temperature distributions inside the heater block (GPHS), and are used to characterize the heat flow distribution.
- Thermocouples 4 and 5 measure the temperature distributions on the wall side and on the vapor side, respectively, of the evaporation interface.
- Thermocouples 6 and 7 measure the temperature distributions on the vapor side and on the wall side, respectively. of the condensation interface.

As seen in Fig. 7, the thermocouples that measure temperature profiles within vapor (5 and 6) are moved through SS304 thermo-sheaths. The O.D. of these thermo-sheaths is 1.82mm (0.072") while the wall thickness was minimized to 0.25mm (0.010") to increase the measurements accuracy. The O.D. of the thermocouples is 1mm (0.040"). The other thermocouples (1-4 and 7) have a 1.65mm (0.065") O.D. The wall thickness of the thermocouples adjacent to the vapor (5 and 6) and the evaporation/condensation surfaces is 0.81mm (0.032"). The distance between the thermo sheaths and the adjacent wall is slightly larger (1mm) to accommodate the presence of the porous structure (screen).
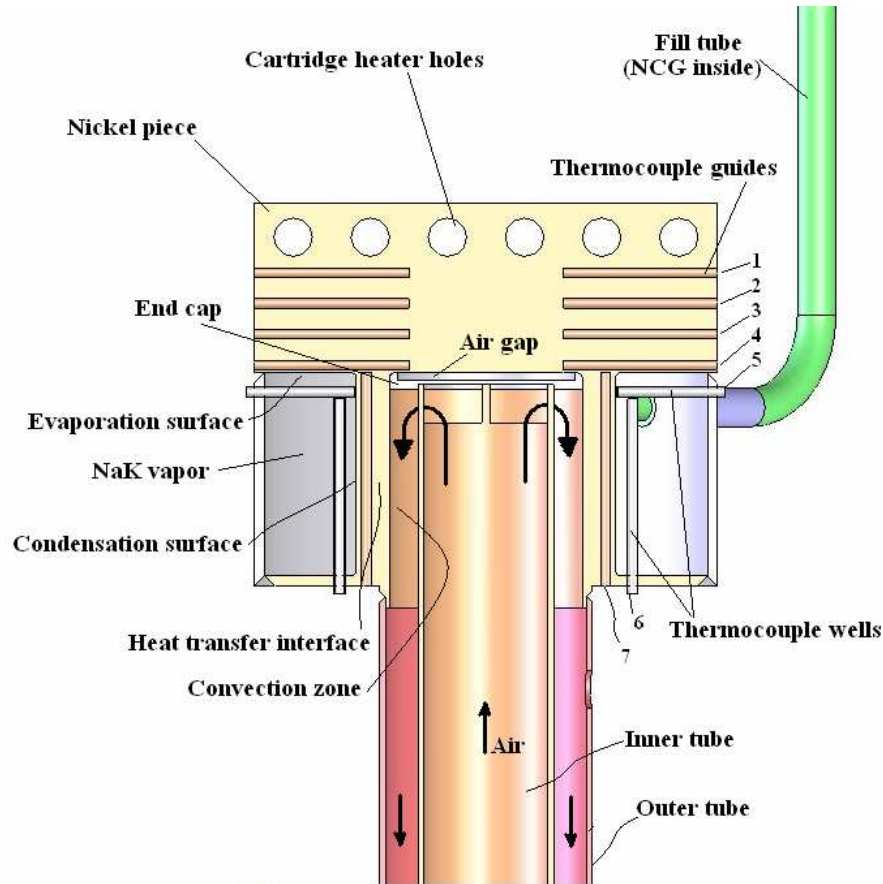
American Institute of Aeronautics and Astronautics

FIGURE 7. NaK behavior test setup – internal details.

A. Heat pipe configuration

The heat pipe for the NaK behavior test setup is wrapped around the heat collector and heater head simulator and has a similar shape and configuration as the VCHP that would be used with an ASRG. The parameters are almost identical, except that the height of the heat transfer zone is approximately 2.2 times larger than the current one in the real ASC. The condenser was lengthened to provide greater resolution during the temperature measurements. The heat pipe was designed to have a controlled amount of non-condensable gas (NCG) to protect the valve at the end of the fill tube (SS304) against the hot vapor (up to 800°C). The NCG was argon, and the number of moles charged into the pipe was calculated so that the vapor-NCG separation interface would be located within the fill tube, 75mm (3") from the heat pipe's wall, for the lowest vapor temperature tested (675°C). The geometrical parameters of the heat pipe in this case are:

- OD = 72.8mm (2.87")
- ID = 42.6mm (1.68")
- IH = 33.5mm (1.32") (inner height)
- screen size – 100 X 100 wires per inch
- number of layers = 3
- total thickness of the screen layer = 0.63mm (0.025")
- porosity of the screen structure = 0.629
- total volume of the screen structure = 1.09E-05 m^3
- void volume within the screen structure = 6.87E-06 m^3
- fill tube total length = 0.292m (11.5")

American Institute of Aeronautics and Astronautics

- fill tube ID = 4.4mm (0.175")
- total volume of the pipe available for NCG after charging with NaK (the thermo-sheaths are taken into account) = 8.07E-05 m^3
- theoretical condensing area = 44.95 cm^2
- theoretical evaporating area = 27.5 cm^2

B. Experimental conditions

The heat pipe is tested with the evaporator above the condenser (against gravity) so that there will be no liquid (excess NaK) on the evaporator surface and no falling liquid film on the condenser surface (see Figures 6 and 7 above). Measurements were carried out for several vapor temperatures between 675 and 800°C. For each vapor temperature, electrical power is applied to the 6 cartridge heaters (connected in parallel) in increments of 100W to generate theoretical heat flux increments of 2.2 W/cm^2 in the condenser, and 3.6 W/cm^2 in the evaporator. As stated before, the heat is applied as a constant power, versus the previous NaK heat pipe tests which used a constant heat flux.

Once a given power is applied to the heaters, the vapor temperature is set by adjusting the coolant mass flow rate until steady state is reached. The flow rate is calculated from the dynamic pressure measured in the center of the inner tube by a Pitot tube (see Fig. 6 above). Additionally, the cooling rate is calculated using the temperatures IN and OUT of the cooling gas measured by the thermocouples shown in Fig. 6. Fourteen temperature profiles are measured by all thermocouples (1-7) on both sides of the testing setup for each vapor temperature – applied power (heat flux) pair. The profiles are measured with a resolution of approximately 4.4mm (0.175"), by manually moving the thermocouples inside their wells/sheaths from the inside toward the outside of the heat pipe.

C. Heat Flux Evaluation

The condenser in the experimental apparatus is 2.2 times longer than the condenser would be in an ASRG with a VCHP. Also, in an ASRG with a VCHP, there would be three layers between the vapor and the inside of the heater head: 1. Haynes 230 for the heat pipe wall, 2. Nickel heat collector, 3. Mar-M 247 heater head wall. In contrast, the experimental apparatus has a thick, high conductivity nickel wall. The other walls were eliminated to avoid any temperature non-uniformities caused by brazing the three walls together.

With a nickel wall, heat can conduct up the nickel wall, so that part of the nickel wall will act like an evaporator rather than a condenser. A CFD analysis examined the effective heat fluxes, and the active condenser fraction as a function of heat flux. This is an approximation, since the binary NaK effects are neglected. However, the analysis showed that the inactive (acts as evaporator) condenser fraction was low for the higher heat fluxes.

The experimental setup was modeled for CFD analysis using the highest experimental vapor temperature, (775°C), since it is closest to the selected ASRG working temperature (850°C). Experimentally, the heat loss with no convective cooling (no gas flow through the heater head simulator) is approximately 155W. The CFD film coefficient boundary conditions were iteratively adjusted until the losses matched the experimental losses. The following values were obtained and used as boundary conditions to simulate the no cooling situation for the 775°**C** vapor temperature case:

- external surface of the heater head simulator: film coefficient h=10 W/m^{2}K, reference temperature T_R=25°C
- all other external surfaces: film coefficient h=7 W/m^{2}K, reference temperature T_R=25°C
- total power (electrical power) = 155 W
- air inlet velocity (coolant velocity) ~ 0 m/s at 25 °C
- air outlet gauge pressure= 0 Pa

These boundary conditions (except total power and inlet velocity) were then used to simulate the experimental conditions corresponding to the other powers (250, 350, 450 and 550W) for the 775°C vapor temperature case. The results of the CFD analysis are presented in Table 2 below.

In the first line of Table 2, the electrical powers (applied to the heaters) are shown. The coolant velocity was varied iteratively, as boundary condition, for each power case until steady state was reached. The cooling power was evaluated by calorimetric calculations. The difference between electrical power in and the cooling power out is the heat lost to the ambient through natural convection. The heat loss to ambient decreases when the electrical power increases since the heat that was lost by conduction to the heater head simulator tubes is now removed by the gas. Table 2 shows the

estimated evaporator and condenser powers. The evaporator power (from wall to vapor) is higher than the power through the condenser (from vapor to wall) due to losses to ambient through the other two walls. Table 2 also shows the location on the "condenser" wall, where the shift in heat flux direction occurs. The area closer to the evaporator surface also acts like an evaporator, due to the heat conducted up the wall. As shown in Table 2, this fraction becomes small (~5%) at the higher heat fluxes.

TABLE 2. Results of the test setup CFD simulation for the 775°C vapor temperature case

Electrical power (heaters) [W]	155	250	350	450	550
Coolant velocity [feet/min]	0	199	496	1048.2	1790
Cooling power [W]	0	130	264	382	509
Power through evaporator [W]	82	158.4	224.64	297.2	374
Power through condenser [W]	31.36	103.6	163.2	230	306.8
Location of heat flux direction change in condenser [cm]	1.4	0.22	0.18	0.172	0.17
Condensing area acting as an Evaporator [%]	44.09%	6.93%	5.67%	5.42%	5.35%
Evaporator area [cm^2]	47.25	30.55	29.98	29.87	29.84
Condenser area [cm^2]	25.12	41.82	42.39	42.50	42.53
Heat flux in the condensing area [W/cm^2]	1.24	2.47	3.85	5.4	7.21

For an actual VCHP-ASRG system, the power fraction transferred through the VCHP (vapor) was calculated as approximately 51% of the power transferred from the GPHS to the heat collector (225W). Assuming that no heat is lost through the two "inactive" or outside walls of the VCHP, the condensing flux in the VCHP-ASRG system is estimated to be 12.8 W/cm^2. The highest heat flux in the current experimental system is 7.21 W/cm^2 due to the longer condenser surface.

III. EXPERIMENTAL RESULTS

Temperature profiles inside the heater block and on both sides of the evaporator surface (in the wall and in the vapor) are shown in Fig. 8 for the two vapor temperature cases (725°C and 775°C) and an electrical power of 550W. The thermocouple numbers shown in the legend correspond to the ones shown in Fig. 7. Near the cartridge heaters, the temperature is fairly uniform except near the exterior wall; see thermocouples 1 and 2. The evaporator surface and vapor temperatures (4 – evaporator wall and 5 – evaporator vapor) are more non-uniform, due to the NaK behavior. Note that the maximum ΔT for each of the four profiles is less than 14°C. Since the last vapor temperature is measured roughly 5.6mm (0.223") away from the exterior, it is possible that the temperature drops further near the exterior wall.
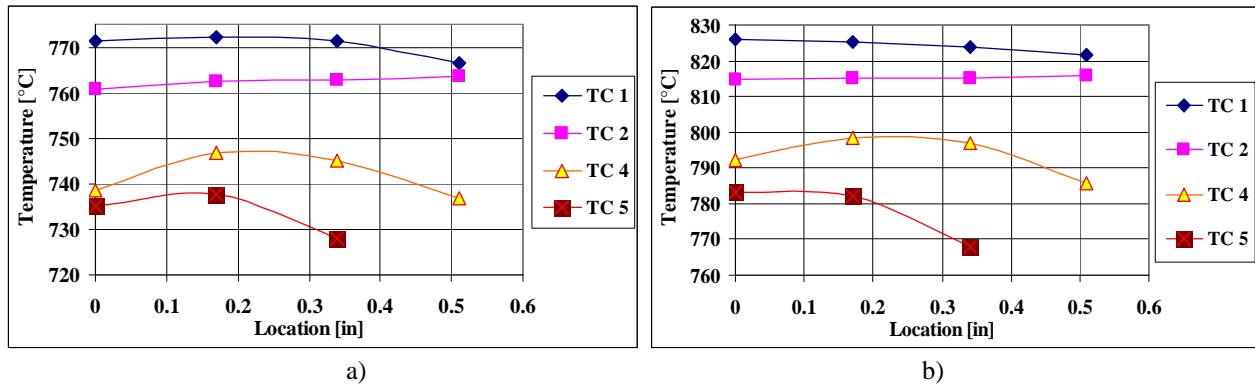

a)   b)

FIGURE 8. Temperature profiles in the heater block and evaporator for a) 725°C and b) 775°C vapor temperature cases and an electrical power of 550 W.

The condenser vapor temperature profiles (measured by thermocouple 6 in Fig. 7) are shown for all six powers below in Fig 9. As expected, the temperature decreases as the probe moves away from the evaporator surface, due to variations in the vapor composition. This occurs since the sodium condenses preferentially as the vapor travels to the

condenser. The more volatile component (K) condenses further away, and at a lower temperature than Na. As a result, the temperature decreases in the downward direction of the setup shown in Fig. 7. The degree of non-uniformity can be simply evaluated as the temperature difference between the two ends of each profile. The temperature differences developed by NaK within the condenser in these two vapor temperature cases are presented in Fig. 10; both wall and vapor measurements are shown.
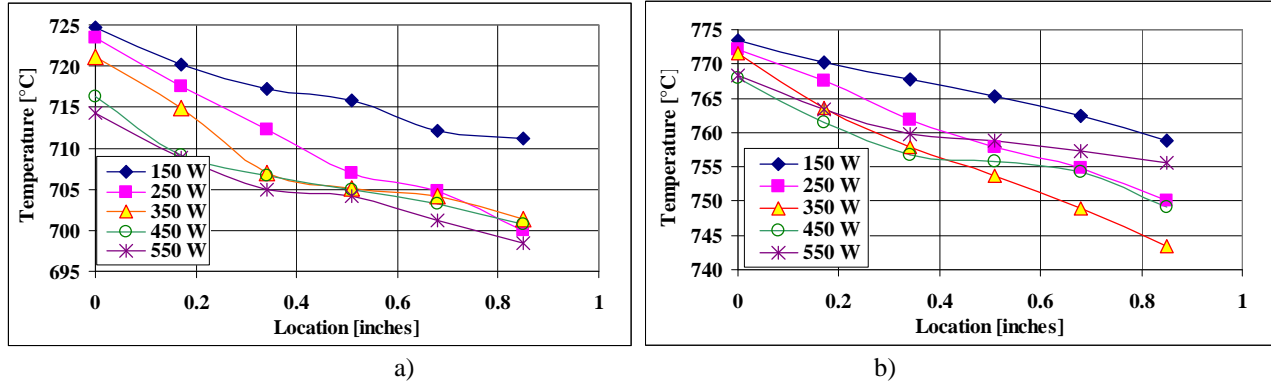

a)   b)

FIGURE 9. **Vapor temperature profiles along the condensation area for a) 725°C vapor temperature case and for b) 775°C vapor temperature case.**

At both vapor temperatures the wall and vapor temperature difference profiles show maxima. The first data point corresponds to the no cooling situation where the so called "condenser" is mostly inactive, with most of the condensation occurring on the outside walls of the heat pipe. As the power increases, the cooling air flow increases, so that most of the condensation occurs on the inner, condenser wall of the heater head simulator. At higher heat fluxes, mixing in the vapor becomes important, discouraging NaK separation, and reducing the ΔT. As expected, the temperature differences developed in the condenser wall are higher than those in the vapor. The temperature difference profile in the wall is in fact a superposition of the temperature difference created by NaK separation with the already existing temperature gradient in the wall due to the heat path.
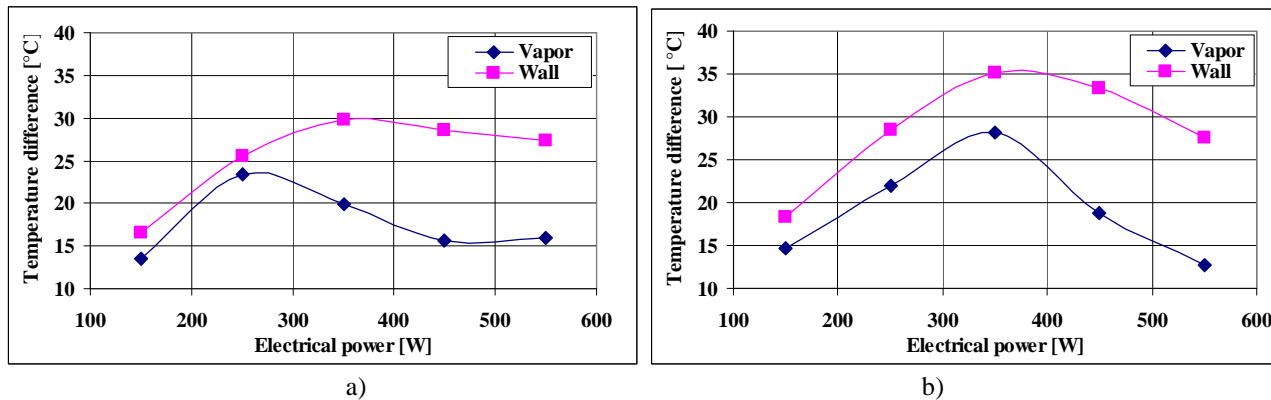

a)   b)

FIGURE 10. **Temperature difference in the condensation area for a) 725°C vapor temperature case and for b) 775°C vapor temperature case.**

The maximum temperature difference developed in all the vapor temperature cases did not exceed 28°C. In addition, this difference did not exceed 16°C for the highest heat flux case (7.21 W/cm^2 at 550W electric power).

The radial temperature differences between condensing vapor and wall, across the condensing interface, are shown above in Fig. 11. This temperature difference gives an indication of the local heat transfer rate. It can be observed that, for the no cooling condition (150 W electrical power applied to the heaters), the direction of the heat flow is dominantly from the wall to the vapor. The other profiles preserve reasonably the expected trend. However, a decrease is observed at the location closest to the outside wall. This might be due to the heat losses to ambient.

10
American Institute of Aeronautics and Astronautics
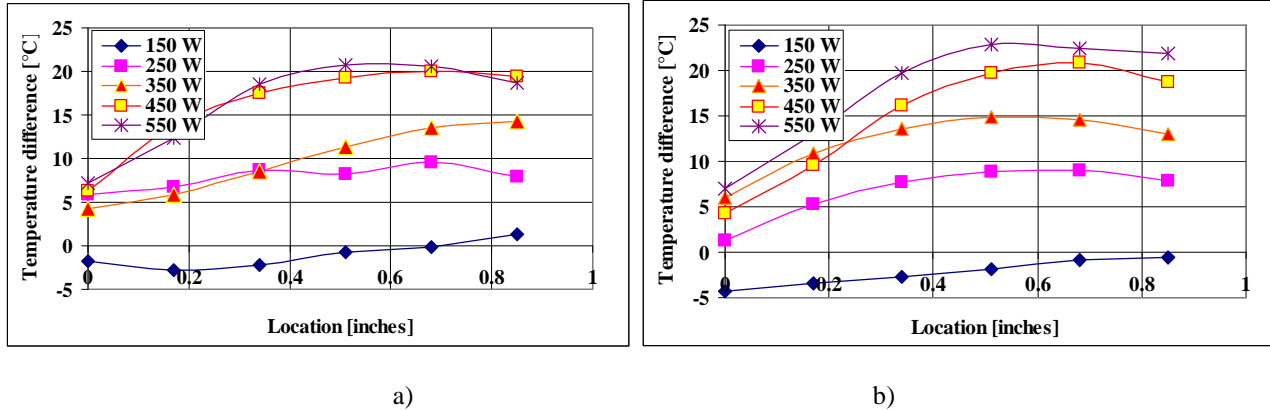
a)　　　　　　　　　　　　　　　　　　b)

FIGURE 11. Temperature difference across the heat transfer interface between vapor and wall, along the condensation area for a) 725°C vapor temperature case and for b) 775°C vapor temperature case.

Temperature difference along the condenser is shown below in Fig. 12 as a function of vapor temperature for all the electrical powers. The general trend observed in both plots (within the vapor and within the wall) is that the temperature difference at constant power increases with vapor temperature. The difference between the vapor pressures of the two components might be the cause. The more volatile potassium vapor pressure increases more rapidly with temperature than sodium vapor pressure. According to the observed trend, an extrapolation would predict an increase of the temperature difference of approximately an additional 5-7°C between 800°C (highest tested temperature) and 850°C (nominal working point of the heater head).
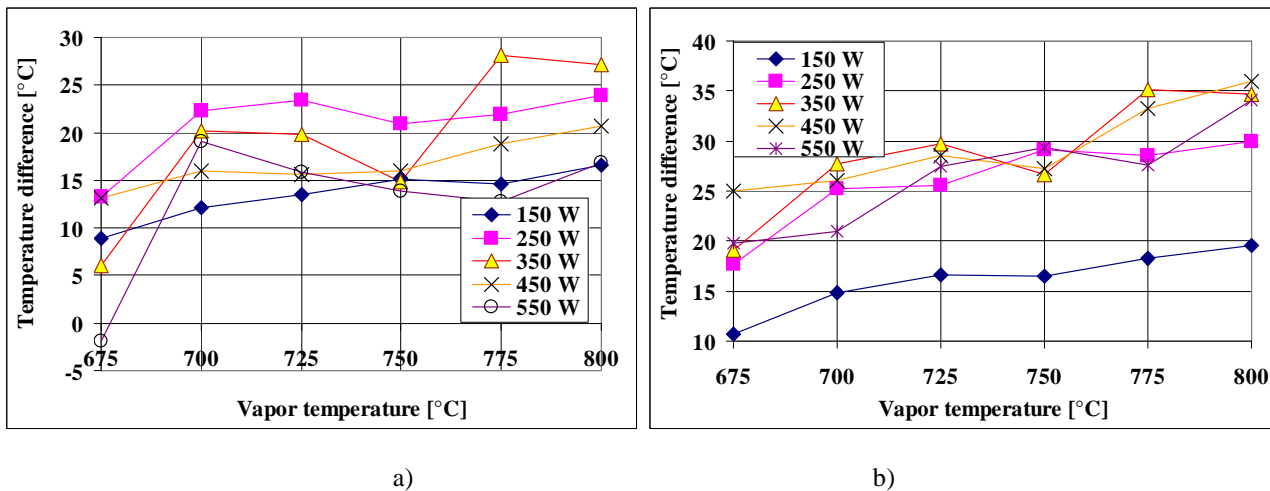

a)　　　　　　　　　　　　　　　　　　b)

FIGURE 12. Temperature differences developed in the condensation area as a function of vapor temperatures within a) vapor and b) wall.

IV. CONCLUSIONS

An alkali-metal Variable Conductance Heat Pipe (VCHP) is under development to allow multiple stops and restarts of the Stirling convertor in the Advanced Stirling Radioisotope Generator (ASRG). Since the VCHP reservoir temperature can vary between 40 and 120°C, NaK is an attractive working fluid because it will not freeze in the reservoir. However, previous NaK heat pipes with constant evaporator heat fluxes have developed large temperature non-uniformities, as high as 80°C, due to distillation of the NaK.

Since the temperature non-uniformities depend on the heat flux and the amount of diffusion of the sodium and potassium in the vapor, a NaK heat pipe with a series of temperature probes was fabricated and tested. The dimensions of the heat pipe are similar to the dimensions of the VCHP for an ASRG, except that the condenser was twice as long.

Constant power was applied rather than constant heat flux, while the region of concern was the condenser rather than the evaporator as in previous NaK testing.

The largest vapor temperature difference observed was 28°C. The temperature non-uniformity decreases when heat flux increases because of mixing enhancement of the sodium and potassium. As heat flux increased to 7.21 W/cm^2, the temperature difference decreased to 16°C for the 775°C vapor temperature case. The temperature differences could be overestimated because of measurement errors. Measurement errors could occur especially at locations close to the exterior wall due to thermal gradients developed in both the thermocouple itself and the thermocouple thermo-sheath. Other factors that increase the temperature difference over what could be expected in a VCHP-ASRG system are that the experimental maximum heat flux for the test results reported here was approximately 60% of the heat flux expected in a VCHP-ASRG system (12.8 W/cm^2) and that the length of the experimental condenser is 2.2 times longer than what would be used in a real VCHP-ASRG system. One adverse effect for an 850 °C VCHP-ASRG system is that the temperature non-uniformities increase with vapor temperature. The potassium vapor pressure increases more rapidly than the sodium vapor pressure, so the ΔT for equal pressure with potassium and sodium increases. The next step is to fabricate and test a complete NaK VCHP.

ACKNOWLEDGMENTS

REFERENCES

Anderson, W. G., Tarau, C., "Variable Conductance Heat Pipes for Radioisotope Stirling Systems", STAIF 2008, Albuquerque, NM, February 10-14, 2008.

Anderson, W. G., Rosenfeld, J. H., and Noble, J., "Alkali Metal Pool Boiler Life Tests for a 25 kWe Advanced Stirling Conversion System," Proceedings of the 26th Annual IECEC, Vol. 5, pp. 343-348, Boston, Mass, August 4-9, 1991.

Anderson, W. G., "Sodium-Potassium (NaK) Heat Pipe," *Heat Pipes and Capillary Pumped Loops*, Ed. A Faghri, A. J. Juhasz, and T. Mahefky, ASME HTD, 236, pp. 47-53, 29th National Heat Transfer Conference, Atlanta, Georgia, August 1993.

Andraka, C. E., Goods, S.H., Bradshaw, R.W., Moreno, J.B., Moss, T.A. and Jones, S.A., "NaK Pool-Boiler Bench-Scale Receiver Durability Test: Test Results And Materials Analysis," 29th IECEC, Monterey, CA, August 7-12 1994.

Chan, T.S., Wood, J. G. and Schreiber, J. G., "Development of Advanced Stirling Radioisotope Generator for Space Exploration," NASA Glenn Technical Memorandum NASA/TM-2007-214806, 2007. http://gltrs.grc.nasa.gov/reports/2007/TM-2007-214806.pdf.

Crockfield, R.D. and Chan, T.S., "Stirling Radioisotope Generator for Mars Surface and Deep Space Missions," Proceedings of 37th Intersociety Energy Conversion Engineering Conference, Washington, D.C., IECEC Paper No. 20188, 2002.

Ernst, D. M., personal communication, 2007.

Rosenfeld, J. H., Ernst, D. M., Lindemuth, J. E., Sanzi, J., Geng, S. M., and Zuo, J., "An Overview of Long Duration Sodium Heat Pipe Tests," NASA Glenn Technical Memorandum NASA/TM—2004-212959, 2004.